World Journal of Applied Physics
2016; 1(1): 16-19
http://www.sciencepublishinggroup.com/j/wjap
doi: 10.11648/j. wjap.20160101.12

Low Level Carbon Detection in Steel Alloys Based on Optimization of Observation Conditions of Laser-Induced Breakdown Spectroscopy (LIBS) in Ambient Air

Mohamed A. Khater

Spectroscopy Department, Physics Division, National Research Centre (NRC), Giza, Egypt

Email address:
drmakhater@gmail.com

To cite this article:
Mohamed A. Khater. Low Level Carbon Detection in Steel Alloys Based on Optimization of Observation Conditions of Laser-Induced Breakdown Spectroscopy (LIBS) in Ambient Air. *World Journal of Applied Physics.* Vol. 1, No. 1, 2016, pp. 16-19.
doi: 10.11648/j.wjap.20160101.12

Received: May 10, 2016; **Accepted**: July 20, 2016; **Published**: August 6, 2016

Abstract: In this study, we present results regarding the application of a relatively simple bench-top laser-induced breakdown spectroscopic (LIBS) technique working in the UV/visible spectral region for the rapid, direct and sensitive quantification of the element carbon in steel alloys under ambient air standard conditions. We carry out further optimization studies and investigate the influence of the gate delay time of the electron multiplier charged-coupled device (EMCCD) detector on the emission properties, namely signal and background intensities as well as signal-to-background ratio (SBR), of the previously selected CI 396.14 nm spectral line. Moreover, we study and compare various methods employed to construct analytical calibration functions of the carbon line under investigation. Furthermore, the analytical figures of merit are evaluated in each case.

Keywords: Detection, Carbon, Steel, LIBS, Air

1. Introduction

The spectroscopic identification and quantification of light elements such as carbon and sulfur within the optical window is a challenge [1]. The problem arises from the fact that strong and well-resolved spectral lines of these elements are originated from their ions and hence essentially located in the vacuum ultraviolet (VUV) spectral regime, where special technical conditions and equipment are required [2-14]. These practices certainly result in preventing the on-line and in-situ applications of the relevant spectroscopic technique.

The situation becomes even more complicated when the host material is mainly composed of a single element-rich-matrix, such as iron in steels, whose spectral lines dominate the UV/visible region. Nevertheless, there has been few published work concerning the direct characterization of steels for their light elements content employing spectroscopic techniques within the readily accessible UV/visible spectral region [15-17]. The results obtained from these studies were however unsatisfactory.

One of the best recognized spectroscopic techniques for the direct and sensitive characterization of materials is laser-induced breakdown spectroscopy (LIBS) [18]. In this technology, a short-lived high-temperature and density plasma plume is generated when a pulsed high-powered laser beam is focused onto a material. The radiation emitted from excited/ionized species in the plasma environment is then spectrally resolved, and the individual neutral atoms and/or atomic ions in the plume are identified and quantified by their unique wavelengths and line intensities, respectively, allowing the characterization of their presence in the parent material [19].

As a part of an ongoing research project, we present in this article results regarding the application of a relatively simple bench-top LIBS technique in the UV/visible spectral regime for the direct, rapid and sensitive quantification of the light element *carbon* in steel alloy targets under ambient air standard conditions. In particular, we carry on our optimization studies and investigate the influence on the emission properties of the previously selected and optimized CI 396.14 nm spectral line of the gate delay time of the electron multiplier charged-coupled device (EMCCD) detector. Furthermore, we also study and compare different methods used to establish analytical calibration functions of this carbon lines and evaluate the corresponding figures of merit in each case.

2. Experimental

A schematic diagram for the LIBS system employed in the present work is depicted in "Fig. 1". In addition, various system components and conditions are described in some details.

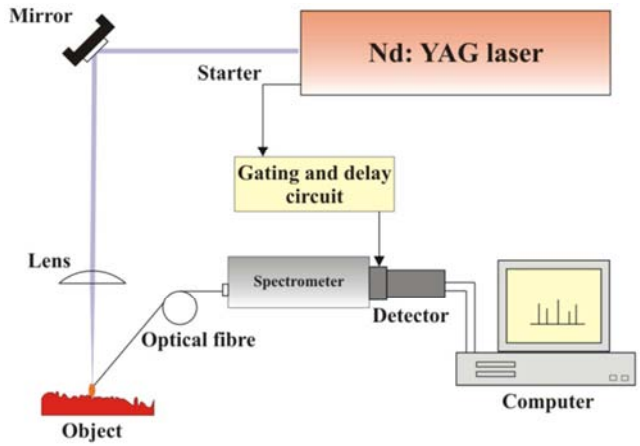

Figure 1. *Experimental set-up.*

Energetic Q-switched Nd:YAG laser pulses (Innolas Laser, model SpitLight Compact 400) with maximum pulse energy of 400 mJ, 6 ns pulse width, 10 Hz repetition rate, and emission wavelength of 1064 nm are focused onto a low alloy steel target in air at atmospheric pressure within a custom-made target chamber. The steel target is mounted on a 3-axis computer controlled translational stages with 75 mm linear travel and 12.5 µm linear resolution.

The smallest radius of the laser beam waist on the steel target was calculated to be 6.0 µm, resulting in a nominal total laser irradiance of 6.0×10^{13} W/cm^2 at 400 mJ pulse energy. The steel target was always kept at 1-2 mm behind the nominal focus of the laser beam in order to prevent accidental air breakdown induced in front of the target surface, which essentially decreases the laser-target coupling and hence ablation efficiency.

All results in this work were obtained by using optimum laser energy value of about 185 mJ at 10 Hz.

The radiation emitted from the laser-generated plasma is collected by a suitable lens and then guided through an attached optical fiber cable, which is in turn connected to a 10 µm×30 µm [W×H] entrance slit of an EMU-120/65 echelle spectrograph (Catalina Scientific). The spectrograph is equipped with UVU3 cassette completed with an aperture stop of 20 mm in diameter.

The dispersed light is detected by an intensfied front illuminated EMCCD (Andor Technology, model iXon3) with 1004×1002 pixel array, and 8 µm×8 µm pixel size. The CCD array has a nominal quantum efficiency of 65% at 600 nm.

All data were recorded by firing 40 successive laser shots onto a specific position of the target surface, which were preceded by 20 burn-in (pre-shots) for cleaning purposes. Measurements were repeated at least 3 times at different locations of the target surface.

The electronic gain of the EMCCD detector was adjusted at an intermediate relative value of 150, and the exposure time (gain width time) of the EMCCD detector was set at an optimum value of 90 µs.

3. Results and Discussion

3.1. Gate Delay Time of the EMCCD Detector

The gate delay time for signal integration of the EMCCD detector is measured from the onset of firing the laser pulse. This is electronically manipulated by a specific control circuit unit designed to link the laser and the detector circuits as shown in Fig. 1. The gate delay time in the current experiments was varied between 1 µs and 10 µs as the lifetime of the neutral species of carbon would last quite long in the plasma. Please note that atomic ions species may have shorter lifetimes, and hence the delay time of the detector would be adjusted at shorter intervals.

Figure 2 illustrates an example of the relationship between the emission properties of the CI 396.14 nm, namely signal as well as background intensities, and the gate delay time of the EMCCD detector.

As can be seen from Fig. 2, the initial emission of both signal and background intensities are very high, as one may expect, with concomitant high levels of uncertainties as well. However, at gate delay times longer than about 1 µs both intensities significantly decrease and almost follow the same behavior. After 2 µs from the onset of laser firing, the emission intensities take a considerable slower rate of decrease all the way down to the last point recorded, i.e. 10 µs.

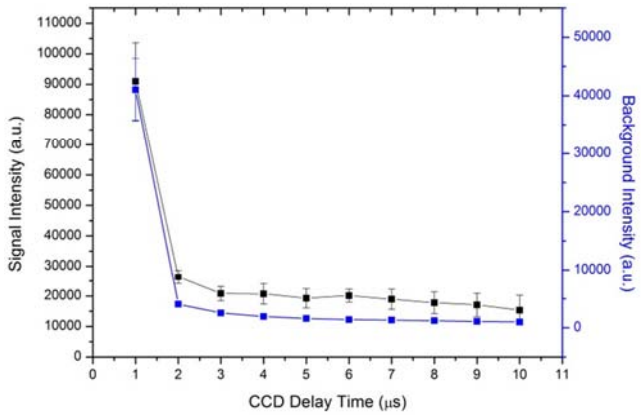

Figure 2. *Signal as well as background intensity of the CI 396.14 nm as a function of the gate delay time of the EMCCD detector.*

The same sets of data points in Fig. 2 were used to calculate the ratio points, and were then again plotted against the gate delay time of the detector. Figure 3 therefore depicts such a relationship between the signal-to-background ratio (SBR) of the CI 396.14 nm spectral line and the gate delay time. As expected, the SBR values increase monotonically with the delay time, then show a leveling off during the 6-10 µs interval.

It is obvious from the figure that the optimum value for the gate delay time of the EMCCD detector is 6 µs. This delay

time does not only provide almost the peak delay value but also proves to be the most stable and reliable as justified by the levels of error bars recorded for higher delay times whose values are almost equal to that at 6 μs.

Figure 4 demonstrates a portion of the UV/visible spectrum of laser-produced steel plasmas recorded at the optimum experimental conditions including that of the EMCCD gate delay time. As can be noted from the figure, the spectrum is naturally dominated by intense neutral Fe spectral lines. Also shown is the carbon line under investigation at 396.14 nm.

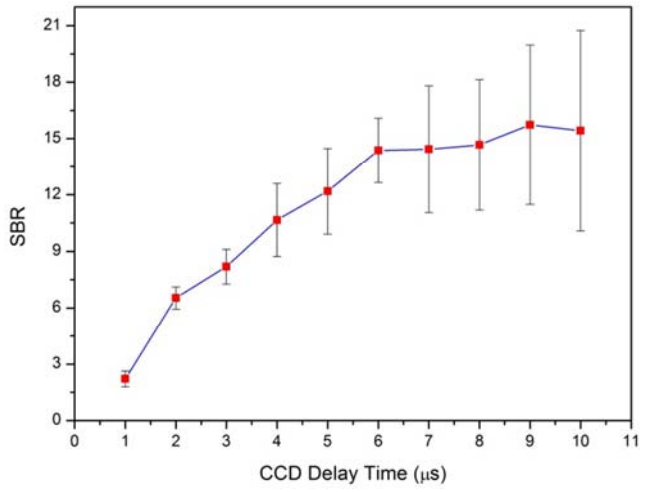

Figure 3. *Signal-to-background intensity ratio of the CI 396.14 nm as a function of the gate delay time of the EMCCD detector.*

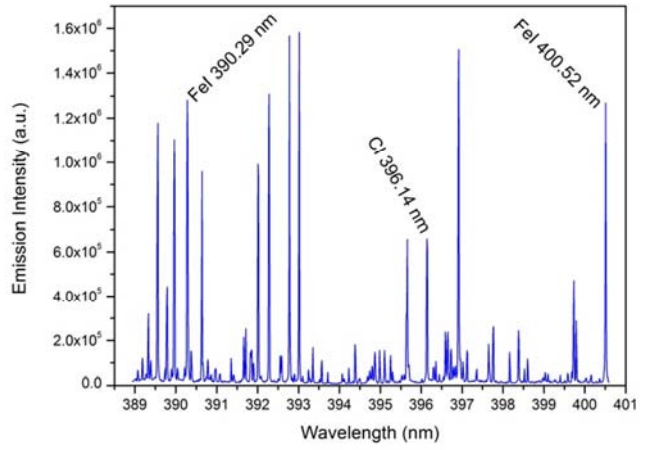

Figure 4. *Portion of an optimized UV/visible spectrum of laser-generated steel plasma in ambient air.*

3.2. Carbon Analytical Functions

Series reference standards of low alloy steel alloy targets containing various concentrations of the element *carbon* are employed in order to inspect the linear relationship between different carbon proportions.

We used the optimum operating conditions and introduced the targets to the laser pulses in succession so that measurements repeated from each target are recorded at different time intervals to ensure that they are subjected to the same conditions, especially those related to fluctuations in the laser energy. All intensity measurements throughout this project were performed by integrating the area under the spectral curve for a specific spectral interval.

Figure 5 illustrates the linear fitting for data points representing the relationship between different concentrations and corresponding integrated intensities for the CI 396.14 nm spectral line. The fitting parameters are also shown including the correlation coefficient factor (R^2) of the linear fitting.

The limit of detection (*LOD*) is a statistical measure of the minimum concentration of an element that the relevant method could detect. In the current experiment, a low ally steel target containing 2.5 ppm carbon was selected to calculate LOD. A limit of detection of about 13.4 ppm ± 1.1 ppm was estimated for *carbon* using the CI 396.14nm spectral line.

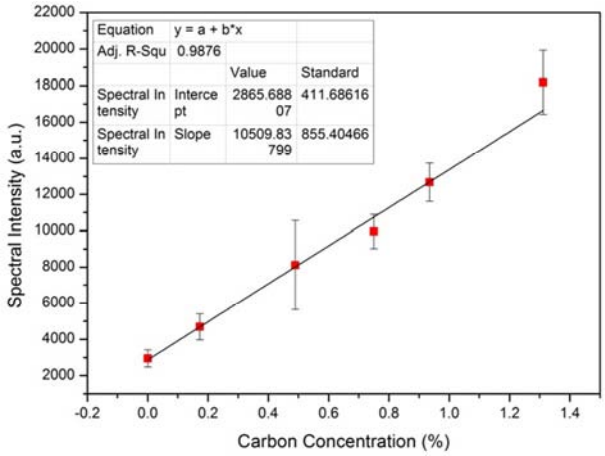

Figure 5. *Linear fitting of the data points used to construct the analytical calibration curve for carbon in steels.*

The data points in Fig. 5 could also be fitted with a polynomial function. Figure 6 depicts the fitting of the data points in Fig. 5 with a 2nd order polynomial function. Although the fitting provider a slightly better correlation as justified by the R^2 value, it yields higher limits of detection due to the high level of uncertainty in the constant B_2. The LOD calculated with this fitting was 16.7 ppm ± 7.1 ppm.

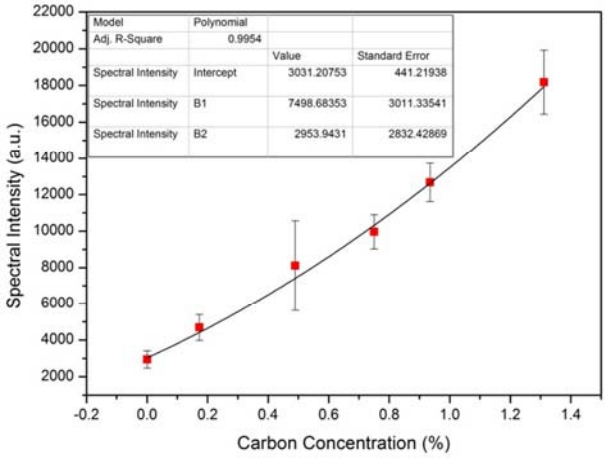

Figure 6. *Polynomial fitting of the data points used to construct the analytical calibration curve for carbon in steels.*

Precision is a measure of the dispersion of the results around a central point represented by the mean value of the measurements. The precision calculated, averaged over the carbon concentration values used to construct the above calibration curve, was estimated at about 8%.

Finally, accuracy is a measure of the difference between a measured concentration to the actual concentration. The average accuracy for concentration measurements was evaluated at about 15%.

4. Conclusion

We studied in some details the influence of the gate delay time for integration of the EMCCD detector within a simple bench-top LIBS technique on the emission properties of the CI 396.14 nm spectral line under ambient air standard conditions. An optimum delay time for the line of interest was found to be 6.0 μs from the onset of firing the laser pulse. In addition, analytical calibration functions for the carbon spectral line were constructed and proved to be linear in the carbon concentration range under investigation. Furthermore, figures of merit of the LIBS technique for this application were evaluated and found to be in favor for the purpose of the current study.

References

[1] M A Khater, Laser-Induced Breakdown Spectroscopy (LIBS) for Light Elements Detection in Steel: State of the Art (invited review), Spectrochim. Acta Part B 81 (2013) 1–10.

[2] J. Aguilera, C. Aragon, J. Campos, Determination of Carbon Content in Steel Using Laser-Induced Breakdown Spectroscopy. Appl. Spectrosc. 46 (1992) 1382–1387.

[3] R. Sattmann, V. Sturm, R. Noll, Laser-Induced Breakdown Spectroscopy of Steel Samples Using Multiple Q-Switch Nd:YAG Laser Pulses, J. Phys. D: Appl. Phys. 28 (1995) 2181–2187.

[4] A. Gonzalez, M. Ortiz, and J. Campos, Determination of Sulfur Content in Steel by Laser-Produced Plasma Atomic Emission Spectroscopy, Appl. Spectrosc. 49 (1995) 1632–1635.

[5] V. Sturm, L. Peter, R. Noll, Steel Analysis with Laser-Induced Breakdown Spectrometry in the Vacuum Ultraviolet, Appl. Spectrosc. 54 (2000) 1275–1278.

[6] M. Khater, P. van Kampen, J. Costello, J-P. Mosnier, E. Kennedy, Time-integrated laser-induced plasma spectroscopy in the vacuum ultraviolet for the quantitative elemental characterization of steel alloys, J. Phys. D: Appl. Phys. 33 (2000) 2252–2262.

[7] M. Hemmerlin, R. Meilland, H. Falk, P. Wintjens, L. Paulard, Application of Vacuum Ultraviolet Laser-Induced Breakdown Spectrometry for Steel Analysis — Comparison with Spark-Optical Emission Spectrometry Figures of Merit. Spectrochim. Acta B 56 (2001), 661–669.

[8] M. Khater, J. Costello, E. Kennedy, Optimization of the Emission Characteristics of Laser-Produced Steel Plasmas in the Vacuum Ultraviolet: Significant Improvements in Carbon Detection Limits, Appl. Spectrosc. 56 (2002) 970–983.

[9] L. Peter, V. Sturm, R. Noll, Liquid Steel Analysis with Laser-Induced Breakdown Spectrometry in the Vacuum Ultraviolet, Appl. Opt. 42 (2003) 6199–6204.

[10] I. Radivojevic, C. Haisch, R. Niessner, S. Florek, H. Becker-Ross, U. Panne, Microanalysis by Laser-Induced Plasma Spectroscopy in the Vacuum Ultraviolet, Anal. Chem. 76 (2004) 1648–1656.

[11] M. Khater, Application of Laser-ablated Plasmas to Compositional Analysis of Steel in the Vacuum Ultraviolet, J. Kor. Phys. Soc. 58 (2011) 1581–1586.

[12] M. Khater, Spatial characteristics of vacuum UV emission from laser–induced plumes in air, Appl. Surf. Sci. 286 (2013) 156–160.

[13] A. A. M. Habib, Calculation of the mean probability of photon capture for vacuum UV line emission of fluorine in the case of a thermal plasma mixture, Spectrochim. Acta Part B 96 (2014) 74–79.

[14] X. Jiang, P. Hayden, J. T. Costello, E. T. Kennedy, Double-pulse laser induced breakdown spectroscopy with ambient gas in the vacuum ultraviolet: Optimization of parameters for detection of carbon and sulfur in steel, Spectrochim. Acta Part B 101 (2014) 106–113.

[15] Y. Ishibashi, Rapid Analysis of Steel by Inductively Coupled Plasma-Atomic Emission Spectrometry and Mass Spectrometry with Laser Ablation Solid Sampling, ISIJ Int. 37 (1997) 885–891.

[16] F. De Lucia, Jr., J. Gottfried, A. Miziolek, Analysis of Carbon and Sulfur in Steel Samples Using Bench Top Laser-Induced Breakdown Spectroscopy (LIBS), General Books LLC, 2011.

[17] C. M. Ahamer, S. Eschlböck-Fuchs, P. J. Kolmhofer, R. Rössler, N. Huber, J. D. Pedarnig, Laser-induced breakdown spectroscopy of major and minor oxides in steel slags: Influence of detection geometry and signal normalization, Spectrochim. Acta Part B 122 (2016) 157–164.

[18] D. Hahn, N. Omenetto, Laser-Induced Breakdown Spectroscopy (LIBS), Part II: Review of Instrumental and Methodological Approaches to Material Analysis and Applications to Different Fields, Appl. Spectrosc. 66 (2012) 347–419.

[19] R. Noll, Laser-Induced Breakdown Spectroscopy: Fundamentals and Applications, first ed., Springer-Verlag, Berlin, 2012.